QUARTERLY JOURNAL OF THE ROYAL METEOROLOGICAL SOCIETY
Q. J. R. Meteorol. Soc. **00**: 1–17 (2007)
Published online in Wiley InterScience
(www.interscience.wiley.com) DOI: 10.1002/qj.000

Representation of 3D heterogeneous cloud fields using copulas: Theory for water clouds

Peter M. Norris[a,b*], Lazaros Oreopoulos[c,d], Arthur Y. Hou[b], Wei-Kuo Tao[d] and Xiping Zeng[a,d]

[a]*Goddard Earth Science and Technology Center, University of Maryland, Baltimore County, Baltimore, Maryland, USA*
[b]*Global Modeling and Assimilation Office, NASA Goddard Space Flight Center, Greenbelt, Maryland, USA*
[c]*Joint Center for Earth Systems Technology, University of Maryland, Baltimore County, Baltimore, Maryland, USA*
[d]*Laboratory for Atmospheres, NASA Goddard Space Flight Center, Greenbelt, Maryland, USA*

Abstract: It is shown that a general representation of GCM column cloud fraction within the PDF-based statistical cloud parameterization context can be obtained by the use of statistical functions called copulas that encapsulate the dependence structure of rank statistics in a multivariate system. Using this theory and cloud resolving model simulations for guidance, a new formulation of GCM cloud overlap is obtained. It is also shown that the use of Gaussian copulas enhances the accuracy of simulating non-linear processes such as the transfer of solar and thermal radiation in multi-layer heterogeneous cloud fields. This first paper, though limited to the simpler case of water clouds, addresses sub-gridscale variability in both moisture and temperature. This work is envisioned to be a first step in developing a generalized statistical framework for transferring information from high-resolution satellite observations into GCMs and global analyses. Copyright © 2007 Royal Meteorological Society

KEY WORDS Statistical cloud parameterizations; Cloud overlap; Cloud heterogeneity; Radiative transfer; Rank statistics

Received 14 September 2007; Revised ; Accepted

1 Introduction

A GCM cloud parameterization typically predicts the cloud fraction and mean cloud properties in each model layer containing cloud. To calculate the radiative impact of these clouds in a GCM column requires the specification of the overlap of the different cloud layers. Early schemes assumed random overlap between model cloud layers, but this suffers from an unphysical dependence on model vertical resolution, and even randomly overlaps adjacent cloudy model layers within the same physical cloud. An improvement is the maximum-random overlap assumption (Tian and Curry, 1989), which assumes maximal overlap between adjacent cloudy layers[1]. However, the scheme still retains some resolution dependence because it relaxes to random overlap between non-contiguous cloud layers, regardless of the thickness of the intervening clear layer. Furthermore, it is reasonable to expect some loss of correlation with height within deeper clouds due to vertical wind shear, for example.

Recently, based on radar observations (Hogan and Illingworth, 2000; Mace and Benson-Troth, 2002) and cloud-resolving model studies (Oreopoulos and Khairoutdinov, 2003; Räisänen *et al.*, 2004; Pincus *et al.*, 2005), a more physical approach has been proposed, called "generalized overlap", in which the combined cloud fraction of any two layers can assume any value between those defined by the extreme assumptions of perfect maximum and random overlap. This is achieved through the introduction of a correlation parameter that can take values between zero for random overlap and one for maximum overlap and whose value drops exponentially as a function of the separation distance between the cloudy layers.

This concept can be also extended to the rank correlation of cloud condensate amount between layers. This governs the likelihood that a large water content in one layer of a GCM column (relative to that layer's water content range) will be paired with a relatively large water content in another layer, and likewise for relatively small water contents. Räisänen *et al.* (2004) and Pincus *et al.* (2005) find that this rank correlation also decreases exponentially with layer separation. The existence of such condensate amount correlations between cloudy layers affects both radiative transfer and precipitation/re-evaporation processes (Jakob and Klein, 1999).

This paper is concerned with formalizing and generalizing these concepts of "generalized overlap" and "condensate rank correlation" within the context of PDF-based statistical cloud parameterizations (e.g., Smith, 1990; Xu and Randall, 1996; Tompkins, 2002; Larson *et al.*, 2001),

*Correspondence to: Dr. Peter Norris, Global Modeling and Assimilation Office, NASA/GSFC, Code 610.1, Greenbelt, MD 20771, USA. Email: peter.m.norris@nasa.gov

[1]The more commonly used variant of the maximum-random overlap scheme due to Geleyn and Hollingsworth (1979) has a somewhat more complicated interpretation. It will not be discussed further in this paper.

which represent the unresolved variabilty within a model gridbox statistically using PDFs (probability density functions). In doing so, we hope to provide a framework for representing realistic three-dimensional sub-gridscale variability in GCM gridcolumns, leading to improved cloud and radiation parameterizations, and as a first step towards transferring the statistical information content of high-resolution satellite cloud observations into GCMs and global analyses.

The paper is organized as follows: Section 2 introduces some key notation, including our primary moisture variable, the total saturation ratio. Section 3 discusses our assumptions, including our initial restriction to the case of water clouds only. It also introduces sub-gridscale statistical distribution functions for layer moisture and temperature. Section 4 introduces the connection between gridcolumn cloud fraction and statistical functions called *copulas*, which we use to describe the rank correlation of saturation ratio between model layers. Section 5 provides a brief introduction to copulas, their utility and properties. Section 6 continues to explore the relationship between cloud fraction and copulas, presenting some simple special cases. Section 7 generalizes our use of copulas to include sub-gridscale temperature variability as well, so that we can move beyond simple cloud fraction evaluation to more complicated gridcolumn quantities, such as radiative fluxes. Section 8 discusses the derivation of the higher order copulas needed to model multi-layer temperature and moisture correlations, and introduces the Gaussian copula in particular. Section 9 obtains a method for inference of Gaussian copula parameters from samples of temperature and moisture within a gridcolumn domain. These samples will be provided by a cloud resolving model (CRM) simulation in this paper, but can be related to high-resolution remote sensing data in the future. Section 10 discusses evaluation of gridcolumn averages within our framework. Section 11 details the generation of random subcolumns from our copula-based framework. Unlike the GCM gridcolumn from which they are drawn, these subcolumns are horizontally uniform and therefore simple to use, but an ensemble of them can approximate the three-dimensional variability of the gridcolumn and so can be used for Monte-Carlo evaluation of gridcolumn mean properties. Subcolumn generators are provided for the Gaussian copula, as well as for simpler random and maximum overlap cases that still retain realistic intra-layer temperature and moisture correlations. Section 12 provides a detailed analysis of the application of our copula-based framework to a single CRM-generated frontally disturbed test case over the ARM (Atmospheric Radiation Measurement) Southern Great Plain site. This preliminary test demonstrates the good performance of the new method for both cloud fraction and radiative property assessment, as compared to random and maximum overlap methods and another more accurate method that preserves the exact geometric overlap of the cloud field but removes inter-layer in-cloud property correlations. Finally, Section 13 summarizes our conclusions and provides a suggested roadmap for practical application of the copula-based framework to GCM cloud and radiation parameterization. We also suggest the assimilation of high-resolution satellite data into GCMs and global analyses as another important potential application of the new framework.

2 Notation

Consider an air parcel of volume V containing masses m_d, m_v and m_c of dry air, water vapor, and water condensate. The corresponding "densities" are $\rho_{d,v,c} \equiv m_{d,v,c}/V$. The "total water density" is $\rho_t \equiv \rho_v + \rho_c$ and the "parcel density" is $\rho \equiv \rho_d + \rho_t$. The partial pressures of dry air and water vapor are $p_d = \rho_d R_d T$ and $e_v = \rho_v R_v T$, where R_d and R_v are the gas constants of water vapor and dry air and T is the parcel temperature. The parcel pressure is $p = p_d + e_v = \rho_* R_d T$, where $\rho_* \equiv \rho_d + \rho_v/\varepsilon$ will be called the "virtual density" and $\varepsilon \equiv R_d/R_v \approx 0.622$.

In this paper we will use "moisture contents"

$$q_{v,c,t} = \rho_{v,c,t}/\rho_*, \tag{1}$$

since the saturation vapor content $q_s \equiv \rho_s/\rho_* = \varepsilon e_s(T)/p$, where $e_s(T)$ is the saturation vapor pressure over a plane pure liquid water surface, has a particularly simple but exact form in this normalization[2].

Next, define the total saturation ratio[3] as

$$S \equiv q_t/q_s, \tag{2}$$

i.e., the total moisture content scaled by the saturation vapor content. This is similar to the "relative humidity", expressed as a fraction, but uses the *total* water content, not the vapor content in the numerator. We will use S instead of q_t in our analysis, since its maximum value will seldom be much in excess of unity. This means that its dynamic range is generally smaller than q_t and it will therefore tend to yield a more well-behaved statistical analysis (see, e.g., Dee and da Silva, 2003).

Finally, note that we will use boldface to represent vectors, e.g., $\boldsymbol{X}$, and San Serif font to represent matrices, e.g., X.

3 Assumptions

This work has an intentionally narrow focus defined by the following assumptions, most of which are quite common in GCM cloud parameterizations:

[2]Vapor and condensate densities are more typically normalized by ρ_d to yield "mixing ratios" $q^{\text{mix}}_{v,c,t} = \rho_{v,c,t}/\rho_d$, or by ρ to yield so-called "specific" quantities $q^{\text{spc}}_{v,c,t} = \rho_{v,c,t}/\rho$. In practice, for the normal atmospheric conditions studied in this paper, ρ_* will seldom be more than a few percent from either ρ_d or ρ, and so there will be rather negligible difference between q^{mix}, q^{spc}, and q. Furthermore, it is a simple matter to convert between these variables. Specifically, $q_{v,c} = q^{\text{mix}}_{v,c}/(1 + q^{\text{mix}}_v/\varepsilon) = q^{\text{spc}}_{v,c}/(1 + \varepsilon' q^{\text{spc}}_v - q^{\text{spc}}_c)$, $q^{\text{mix}}_{v,c} = q_{v,c}/(1 - q_v/\varepsilon)$ and $q^{\text{spc}}_{v,c} = q_{v,c}/(1 - \varepsilon' q_v + q_c)$, where $\varepsilon' \equiv 1/\varepsilon - 1$.

[3]Or just the "saturation ratio".

DOI: 10.1002/qj

(A1) Consider a single GCM gridcolumn, or a contiguous vertical section thereof, comprised of K layers, numbered $k = 1 \ldots K$, top to bottom. Assume each layer to be sufficiently shallow that *all* its properties can be taken as *vertically* uniform. Clearly this is unphysical for pressure, but assume that no significant error is made by using the layer mid-point pressure in all calculations that follow.

(A2) Assume the layer pressure p is also horizontally uniform, whereas the layer temperature T and saturation ratio S are horizontally non-uniform[4] and distributed according to cumulative distribution functions F_{T_k} and F_{S_k} for layer k. Specifically, $F_{T_k}(t)$ and $F_{S_k}(s)$ are the fractions of the layer volume for which $T_k \leq t$ and $S_k \leq s$. By assumption (A1), these volume fractions are identical to the respective areal fractions of the layer, as seen from directly above (i.e., from zenith). We therefore employ the shorthand $F_{T_k}(t) = \mathrm{Fr}(T_k \leq t)$ and $F_{S_k}(s) = \mathrm{Fr}(S_k \leq s)$, where $\mathrm{Fr}(A)$ is the areal fraction of the gridcolumn, as viewed from zenith, for which condition A holds. Note that F_{T_k} is non-decreasing and has $F_{T_k}(0) = 0$ and $F_{T_k}(\infty) = 1$, and similarly for F_{S_k}. We further assume that both F_{T_k} and F_{S_k} are continuous.

(A3) We restrict our attention to contiguous vertical sub-sections of a grid-column that contain only liquid phase condensate and for which each contained layer has $T \geq 0°\mathrm{C}$ everywhere. We make this assumption in order to simplify development of our basic theory, as discussed in (A4) below. We will include mixed phase and ice clouds in a future paper.

(A4) Assume that q_v nowhere exceeds its saturation value $q_s = \varepsilon e_s(T)/p$, and that any excess water is present as condensed liquid water $q_c = (q_t - q_s)H(q_t - q_s) = (S-1)q_s H(S-1)$, where H is the Heaviside step function. This so-called "bulk condensate" assumption is often used in GCMs, since in most warm clouds vapor supersaturations are very small[5]. This partially explains why we have limited this paper to liquid water clouds — in ice clouds, supersaturations in excess of 10% or 20% are often seen.

[4]Previous work (e.g., Tompkins, 2002) has often included sub-gridscale variability in moisture only, not in temperature. From a study of aircraft observations of liquid water clouds, Tompkins (2003) finds that the errors in cloud fraction caused by neglect of sub-gridscale temperature variability are about half those caused by the neglect of sub-gridscale moisture variability. Tompkins concludes that for a zero-order treatment of sub-gridscale variability it may be acceptable to treat moisture variability alone, but that inclusion of temperature variability should be a goal in future statistical parameterizations. We therefore include temperature variability from the outset.

[5]In reality, cloud condensate is composed of hydrometeors which may or may not be instantaneously in equilibrium with the surrounding vapor field. Nevertheless, at least for a typical warm cloud condition, our calculations with a microphysical droplet growth model indicate such equilibrium typically occurs within a minute, much shorter than the typical timestep for GCM phase change routines. The situation for ice-phase clouds is definitely more complicated, and will be addressed in a future paper. For the liquid water clouds currently under consideration, assume that the liquid phase is in equilibrium with the vapor field, and that curvature and solute effects, which lead to departures of the saturation vapor pressure from that over a plane pure liquid surface, are not significant in the bulk, hydrometeor-size-integrated sense.

4 Cloud Fraction and Copulas

4.1 Definition of Clear/Cloud Fraction

Define the *clear fraction* f'_k of layer k as the areal fraction of the layer, when viewed from zenith, which has zero condensate at any level within the layer. This is technically an *areal* clear fraction, but under the shallow layer assumption (A1) it is identical to the so-called *volumetric* clear fraction, which is the fractional volume of the layer with zero condensate. We will therefore drop the prefix "areal" or "volumetric" and speak only of the clear fraction f'_k. Using assumptions (A1) ...(A4), we may therefore write:

$$f'_k = \mathrm{Fr}(q_{tk} \leq q_{sk}) = \mathrm{Fr}(S_k \leq 1) = F_{S_k}(1). \quad (3)$$

The corresponding *cloud fraction* is just $f_k \equiv 1 - f'_k$.

The *column clear fraction* f' is likewise defined as the areal fraction of the entire gridcolumn, as viewed from zenith, which has zero condensate at any level. The determination of f' is a major subject of this paper. The *column cloud fraction* f is likewise defined by $f \equiv 1 - f'$.

Why is f' an interesting quantity to evaluate and study? Apart from being mathematically interesting quantity, f' has been used extensively in the past in simple plane parallel radiative transfer schemes as a proxy for the portion of a GCM gridcolumn unaffected by cloud. Also, from a satellite data assimilation perspective, f' is related (albeit imperfectly) to the fraction of pixels in a region that are not "masked" as cloudy, a common product of many satellite cloud retrievals. In the real world there are many complicating issues: the existence of sideways photon transport in broken cloud fields, the occurance of non-zenith solar and satellite viewing angles, etc. Nevertheless, for a start, we wish to explore the determination of f' under the assumptions discussed above and for the simple reasons just outlined. It will also turn out, as we proceed, that our analysis can be used to model complex inter-variable and inter-layer correlations within a gridcolumn, and will therefore have far wider application to GCM parameterization and data assimilation than our initial focus on column cloud fraction suggests.

4.2 Formal Evaluation

Let $F_{\boldsymbol{S}}$, where $\boldsymbol{S} \equiv (S_1, \ldots, S_K)^T$, be the joint cumulative distribution function of saturation ratio for all layers in the gridcolumn. Specifically, $F_{\boldsymbol{S}}(\boldsymbol{s}) = \mathrm{Fr}(S_1 \leq s_1, \ldots, S_K \leq s_K)$, where $\mathrm{Fr}(A, B)$ means $\mathrm{Fr}(A \cap B)$. $F_{\boldsymbol{S}}$ has the properties that it is K-increasing[6] and that

[6]"K-increasing" in this context means that $V_{F_{\boldsymbol{S}}}(B) \geq 0$ for any K-dimensional box $B = [\boldsymbol{a}, \boldsymbol{b}] = [a_1, b_1] \times \ldots \times [a_K, b_K]$ in $[0, \infty]^K$ with $\boldsymbol{a} \leq \boldsymbol{b}$ (i.e., $a_1 \leq b_1, \ldots, a_K \leq b_K$), where $V_{F_{\boldsymbol{S}}}(B) \equiv \Delta_{a_K}^{b_K} \ldots \Delta_{a_1}^{b_1} F_{\boldsymbol{S}}$ and

$$\Delta_{a_k}^{b_k} F_{\boldsymbol{S}}(\boldsymbol{s}) \equiv F_{\boldsymbol{S}}(s_1, \ldots, s_{k-1}, b_k, s_{k+1}, \ldots, s_K) - F_{\boldsymbol{S}}(s_1, \ldots, s_{k-1}, a_k, s_{k+1}, \ldots, s_K).$$

The joint cumulative distribution $F_{\boldsymbol{S}}$ defined above *is* K-increasing, since for it to be otherwise would imply that there existed some B which contained a *negative* areal fraction.

DOI: 10.1002/qj

$F_{\boldsymbol{S}}(\boldsymbol{s}) = 0$ if at least one coordinate of $\boldsymbol{s}$ is zero and $F_{\boldsymbol{S}}(\infty, \ldots, \infty) = 1$. Then, using the above definitions,

$$f' = F_{\boldsymbol{S}}(1, \ldots, 1). \tag{4}$$

Define the "k-th margin" of $F_{\boldsymbol{S}}(\boldsymbol{s})$ as the one-dimensional function obtained from it by setting $s_i = \infty \, \forall \, i \neq k$. From the definition of $F_{\boldsymbol{S}}$ we see that its k-th margin is none other than the cumulative distribution function of layer k alone, i.e., F_{S_k} [see (A2)].

Then, by **Sklar's Theorem** (see Nelson, 2006, Theorem 2.10.9), $\exists$ a unique "K-copula" $C_{\boldsymbol{S}}$ (to be defined shortly) such that $\forall \, \boldsymbol{s} \in [0, \infty]^K$,

$$F_{\boldsymbol{S}}(\boldsymbol{s}) = C_{\boldsymbol{S}}(F_{S_1}(s_1), \ldots, F_{S_K}(s_K)). \tag{5}$$

Then, by (4) and (3), we may write

$$f' = C_{\boldsymbol{S}}(F_{S_1}(1), \ldots, F_{S_K}(1)) = C_{\boldsymbol{S}}(f'_1, \ldots, f'_K). \tag{6}$$

Hence, we see that this K-copula $C_{\boldsymbol{S}}$, which we shall investigate shortly, is the special function which converts the set of layer clear fractions $\{f'_k\}$ to the gridcolumn clear fraction f'.

5 Copulas

What is a copula? From (5), it is a function which joins a joint cumulative distribution function to its one-dimensional margins. It describes the scale-free dependence among a set of variables in the sense that it is a joint cumulative distribution function of the *ranks* of the variables within their respective distributions.

The theory of copulas is discussed extensively in a monograph by Nelson (2006), which includes the following formal definition: A K-copula is a function C from $\boldsymbol{I}^K$ to $\boldsymbol{I}$ (where $\boldsymbol{I} \equiv [0, 1]$) with the following properties:

1. $\forall \, \boldsymbol{r} = (r_1, \ldots, r_K)^T \in \boldsymbol{I}^K$,
   $C(\boldsymbol{r}) = 0$ if at least one coordinate of $\boldsymbol{r}$ is 0, and
   $C(\boldsymbol{r}) = r_k$ if all coordinates of $\boldsymbol{r}$ are 1 except r_k;
2. $\forall \, \boldsymbol{a}, \boldsymbol{b} \in \boldsymbol{I}^K$ such that $\boldsymbol{a} \leq \boldsymbol{b}$, $V_C([\boldsymbol{a}, \boldsymbol{b}]) \geq 0$,

where the K-box volume function V_C and other notation was defined earlier[6].

The following are various results from copula theory which we will use:

(R1) Two simple copulas with special significance in copula theory are the "product copula" $\Pi^K(\boldsymbol{r}) = \prod_{k=1}^K r_k$ and the "M copula" $M^K(\boldsymbol{r}) = \min(r_1, \ldots, r_K)$.

(R2) The $\binom{K}{k}$ "k-margins" of a K-copula C, formed by setting $K - k$ of the arguments of C to one, are k-copulas.

6 Special Cases

In our context, item (R2) implies that if only K^* of the K layers are cloudy (i.e., have $f'_k < 1$), then (6) reduces to

$$f' = C^*_{\boldsymbol{S}}(f'_{k^*_1}, \ldots, f'_{k^*_{K^*}}), \tag{7}$$

where the k^* are the cloudy layer indices and the copula $C^*_{\boldsymbol{S}}$ is the K^*-margin of $C_{\boldsymbol{S}}$ formed by marginalizing all the clear layers. Marginalizing the clear layers is equivalent to ignoring them and $C^*_{\boldsymbol{S}}$ is just the copula of the variability of the cloudy layers only. Hence, we can retain all our previous results, such as (6), if we (a) redefine the "gridcolumn" as the subset of cloudy layers only, (b) redefine K as the number of cloudy layers, which we relabel $k = 1 \ldots K$, and (c) completely ignore clear layers. Then $F_{\boldsymbol{S}}$ and $C_{\boldsymbol{S}}$ represent the joint cumulative distribution function and copula for cloudy layers only, but f' *remains* the *total* column clear fraction, since clear layers have no influence on f'.

More generally, all our previous results also apply to *any* subset of the gridcolumn layers, so long as we redefine K as the number of such layers, relabeled $k = 1 \ldots K$, and so long as we regard f' as the column clear fraction associated with that subset of layers only, effectively treating any layers outside of the subset as non-existent.

6.1 Simple Cases

Two common special cases of (6) are:

1. If all layers are completely independent we will have $f' = \prod_{k=1}^K f'_k$, which corresponds to $C_{\boldsymbol{S}} = \Pi^K$, the "product copula". This leads to the so-called "random overlap" cloud fraction

$$f_{\text{RAN}} = 1 - \prod_{k=1}^{K} f'_k. \tag{8}$$

   Random overlap is unrealistic when applied to closely separated model layers within a contiguous cloud layer.

2. If $C_{\boldsymbol{S}} = M^K$, the "M copula", then we obtain $f' = \min(f'_1, \ldots, f'_K)$ and the so-called "maximum overlap" cloud fraction

$$\begin{aligned} f_{\text{MAX}} &= 1 - \min(f'_1, \ldots, f'_K) \\ &= \max(f_1, \ldots, f_K). \end{aligned} \tag{9}$$

   Though more realistic than random overlap when applied within a cloud, we do expect some transition towards random overlap between distant model layers within a deep cloud.

Appendix A gives an example to the combination of these different cloud fraction copulas for the case of multiple cloud layers.

DOI: 10.1002/qj

7 The Joint Distribution of T and S

So far we have a way of evaluating the layer and column cloud fractions using (3) and (6) via the statistical properties of $\boldsymbol{S}$. But we also need a way characterize the *joint* distributions of $\boldsymbol{T}$ and $\boldsymbol{S}$ so that we may estimate more complex quantities than cloud fraction, such the radiative or preciptation forming properties of a collection of cloud layers, which depend on a knowledge of $\boldsymbol{T}$, $\boldsymbol{q_v}$ and $\boldsymbol{q_c}$, among others. Let $F_{\boldsymbol{T},\boldsymbol{S}}$ be the joint distribution function of $\boldsymbol{T}$ and $\boldsymbol{S}$. Then by Sklar's Theorem $\exists$ a unique $2K$-copula $C_{\boldsymbol{T},\boldsymbol{S}}$ such that $\forall\, \boldsymbol{t}, \boldsymbol{s} \in [0,\infty]^K$,

$$\begin{aligned} F_{\boldsymbol{T},\boldsymbol{S}}(\boldsymbol{t},\boldsymbol{s}) = C_{\boldsymbol{T},\boldsymbol{S}}(&F_{T_1}(t_1),\ldots,F_{T_K}(t_K),\\ &F_{S_1}(s_1),\ldots,F_{S_K}(s_K)). \end{aligned} \tag{10}$$

Note that the saturation ratio K-copula $C_{\boldsymbol{S}}$ of (5) is just the K-margin of $C_{\boldsymbol{T},\boldsymbol{S}}$ that marginalizes the temperatures. Namely,

$$C_{\boldsymbol{S}}(r_1,\ldots,r_K) = C_{\boldsymbol{T},\boldsymbol{S}}(1,\ldots,1,r_1,\ldots,r_K). \tag{11}$$

8 Multivariate Copulas

There are numerous bivariate copulas discussed in Nelson (2006). However, in order to model the cloud overlap properties of multiple layers, we need to find suitable copulas of higher order. Unfortunately, it is usually not possible to extend a bivariate copula to higher dimensions while retaining the flexibility it has in two dimensions.

There are several different approaches to building copulas of order three and above. One strategy (Chakak and Koehler, 1995) starts with bivariate marginal copula and uses conditional probability arguments to iteratively construct higher order margins that include the lower order ones but also capture the joint rank dependence of progressively larger numbers of layers. We have not found this method easy to use and will not discuss it further.

The approach we will take is to investigate transformations of $(\boldsymbol{T},\boldsymbol{S})$ space that yield known multivariate distribution functions. These analytic $F_{\boldsymbol{T},\boldsymbol{S}}$ then translate to analytic copulas via Sklar's Theorem (10).

8.1 Transformed Multinormal Distributions and the Gaussian Copula

Suppose there exist *monotonic increasing* transformations

$$\left.\begin{aligned} Z_{Tk} &= G_{Tk}(T_k)\\ Z_{Sk} &= G_{Sk}(S_k) \end{aligned}\right\},\ k \in \{1,2,\ldots,K\}, \tag{12}$$

such that $\boldsymbol{Z} \equiv (Z_{T1},...,Z_{TK},Z_{S1},\ldots,Z_{SK})^T \in \mathbb{R}^{2K}$ has a multivariate Normal (i.e., multinormal) distribution with zero mean ($\mathrm{E}(\boldsymbol{Z}) = \boldsymbol{0}$) and covariance $\mathsf{C} = \mathrm{E}[\boldsymbol{Z}\boldsymbol{Z}^T]$, or using common statistical shorthand, $\boldsymbol{Z} \sim N_{2K}(\boldsymbol{0},\mathsf{C})$, and that C has unit variances (ones on its diagonal) and is therefore a correlation matrix[7]. The implication of these transformations is that the density of areal fraction in $\boldsymbol{Z}$ space is

$$p_{\boldsymbol{Z}}(\boldsymbol{z};\mathsf{C}) = (2\pi)^{-K}|\mathsf{C}|^{-1/2}\exp\{-\boldsymbol{z}^T\mathsf{C}^{-1}\boldsymbol{z}/2\}. \tag{13}$$

Using the monotonic increasing property of the G_k,

$$\begin{aligned} &F_{\boldsymbol{T},\boldsymbol{S}}(\boldsymbol{t},\boldsymbol{s})\\ &\quad= \mathrm{Fr}(T_1 \le t_1,\ldots,T_K \le t_K,\\ &\qquad S_1 \le s_1,\ldots,S_K \le s_K)\\ &\quad= \mathrm{Fr}(Z_{T1} \le G_{T1}(t_1),\ldots,Z_{TK} \le G_{TK}(t_K),\\ &\qquad Z_{S1} \le G_{S1}(s_1),\ldots,Z_{SK} \le G_{SK}(s_K))\\ &\quad= F_{\boldsymbol{Z}}(G_{T1}(t_1),\ldots,G_{TK}(t_K),\\ &\qquad G_{S1}(s_1),\ldots,G_{SK}(s_K);\mathsf{C}), \end{aligned} \tag{14}$$

where

$$F_{\boldsymbol{Z}}(z_1,\ldots,z_{2K};\mathsf{C}) = \int_{-\infty}^{z_1}\cdots\int_{-\infty}^{z_{2K}} p_{\boldsymbol{Z}}(\boldsymbol{z}';\mathsf{C})d\boldsymbol{z}'. \tag{15}$$

There is no closed form for the multinormal distribution $F_{\boldsymbol{Z}}$, so it must be evaluated numerically. Such methods exist, for example, Genz (1992) and a related MATLAB implementation by Alex Strashny (http://alex.strashny.org/b/mvncdf.m).

That there exist these transformations G_k yielding $\boldsymbol{Z} \sim N_{2K}(\boldsymbol{0},\mathsf{C})$ is an assumption. If this assumption is not valid we shall be essentially fitting $(\boldsymbol{T},\boldsymbol{S})$ with a transformed multinormal, and seeking those parameters which give the best fit. Anyway, assuming $\boldsymbol{Z} \sim N_{2K}(\boldsymbol{0},\mathsf{C})$, it is a property of the multinormal that each of the $2K$ margins is normally distributed as $Z_k \sim N(0,\mathsf{C}_{kk}) = N(0,1)$, i.e., each Z_k is a standard normal variate.

Since Z_{Tk} and Z_{Sk} are $\sim N(0,1)$,

$$\begin{aligned} F_{Z_{Tk}}(z) = F_{Z_{Sk}}(z) &= \frac{1}{2}\left[1 + \mathrm{erf}\left(\frac{z}{\sqrt{2}}\right)\right]\\ &\equiv \Phi(z), \end{aligned} \tag{16}$$

which is the standard Normal cumulative distribution function. Its inverse is

$$\Phi^{-1}(p) = \sqrt{2}\ \mathrm{erf}^{-1}(2p-1). \tag{17}$$

Since G_{Tk} is monotonic increasing,

$$\begin{aligned} F_{T_k}(t) &= \mathrm{Fr}(T_k \le t) = \mathrm{Fr}(Z_{Tk} \le G_{Tk}(t))\\ &= F_{Z_{Tk}}(G_{Tk}(t)) = \Phi(G_{Tk}(t)), \end{aligned}$$

and similarly for G_{Sk}, so that

$$\begin{aligned} G_{Tk}(t) &= \Phi^{-1}(F_{T_k}(t)) \quad \text{and}\\ G_{Sk}(s) &= \Phi^{-1}(F_{S_k}(s)). \end{aligned} \tag{18}$$

[7]For the existence of such transformations we actually require only that there exist monotonic increasing transformations such that $\boldsymbol{Z}$ has an arbitrary multinormal distribution, i.e., $\boldsymbol{Z} \sim N_{2K}(\boldsymbol{\mu},\boldsymbol{\Sigma})$, except only that $\boldsymbol{\Sigma}$ has all non-zero variances $\sigma_k^2 \equiv \boldsymbol{\Sigma}_{kk} > 0$, since then the further monotonic increasing transformations $(Z_k - \mu_k)/\sigma_k \mapsto Z_k$, yield $\boldsymbol{Z} \sim N_{2K}(\boldsymbol{0},\mathsf{C})$, where C is the correlation matrix $\mathsf{C}_{ij} \equiv \boldsymbol{\Sigma}_{ij}/(\sigma_i\sigma_j)$.

DOI: 10.1002/qj

Combining these with (14), we have

$$F_{\boldsymbol{T},\boldsymbol{S}}(\boldsymbol{t},\boldsymbol{s}) = C_{\boldsymbol{Z}}(F_{T_1}(t_1),\ldots,F_{T_K}(t_K), F_{S_1}(s_1),\ldots,F_{S_K}(s_K);\mathsf{C}), \tag{19}$$

as in (10), with

$$C_{\boldsymbol{Z}}(r_1,\ldots,r_{2K};\mathsf{C}) = F_{\boldsymbol{Z}}(\Phi^{-1}(r_1),\ldots,\Phi^{-1}(r_{2K});\mathsf{C}), \tag{20}$$

$\forall r_k \in [0,1]$. This $C_{\boldsymbol{Z}}$ is the so-called "Gaussian copula" (e.g., Cherubini *et al.*, 2004) and can be used in place of $C_{\boldsymbol{T},\boldsymbol{S}}$. Once the $K(2K-1)$ unique elements of the correlation matrix C are specified, we can evaluate the column clear fraction f' using (11) and (6). Or if we know the form of the $2K$ single layer margins F_{T_k} and F_{S_k}, we can evaluate the full joint distribution $F_{\boldsymbol{T},\boldsymbol{S}}$ using (19). In either case, the result will only be as good a our assumption that the $(\boldsymbol{T},\boldsymbol{S})$ field is a transformed multinormal. If it is not, we can adjust C and the parameters of the F_{T_k} and F_{S_k} distributions to give the best fit to the observed cloud fraction or $(\boldsymbol{T},\boldsymbol{S})$ data.

9 Inference of Copula Parameters

Say we are supplied with N random samples $\{\boldsymbol{T}^{(1)},\ldots,\boldsymbol{T}^{(N)}\}$ and $\{\boldsymbol{S}^{(1)},\ldots,\boldsymbol{S}^{(N)}\}$ from a grid-column and wish to model the scale-free dependence between layers using copulas. We will assume here that the marginal distributions F_{T_k} and F_{S_k} are known exactly or have been estimated in a prior step. Then the sample ranks are given by

$$R_k^{(n)} = \begin{cases} F_{T_k}(T_k^{(n)}), & \text{for } k = 1,\ldots,K, \text{ and} \\ F_{S_k}(S_k^{(n)}), & \text{for } k = K+1,\ldots,2K. \end{cases} \tag{21}$$

Also, suppose we have a candidate analytic copula, $C(r_1,\ldots,r_{2K};\boldsymbol{\alpha})$, with parameters $\boldsymbol{\alpha}$, that we wish to use to model the interdependence between the layer ranks. We now desire a method of estimating some "best fit" value of $\boldsymbol{\alpha}$, call it $\hat{\boldsymbol{\alpha}}$, from the supplied $R_k^{(n)}$.

One approach is to seek a maximum likelihood estimate (MLE) of $\boldsymbol{\alpha}$. Our preliminary investigations of this problem, for the simple case of the Gaussian copula, have not been at all trivial. Furthermore, it is well known that maximum likelihood estimates are not necessarily unbiased estimates, namely that the expected values of the estimated parameters are not necessarily equal to the parameters of the population from which the samples were drawn. It is important to have unbiased parameter estimates so that further generation of samples from the copula (see §11) will be as consistent with the underlying population as possible. For these reasons, we seek an *unbiased* estimate of $\boldsymbol{\alpha}$.

We will limit our investigation to the simple case of the Gaussian copula, so we seek an unbiased estimate $\hat{\mathsf{C}}$ of the correlation matrix of the distribution $\boldsymbol{Z} \equiv (\Phi^{-1}(R_1),\ldots,\Phi^{-1}(R_{2K}))^T \sim N_{2K}(\boldsymbol{0},\mathsf{C})$ underlying the Gaussian copula. It is well known that an unbiased estimate of C is provided by the "sample covariance matrix"

$$\Sigma^*_{ij} \equiv \sum_{n=1}^{N} (Z_i^{(n)} - \bar{Z}_i)(Z_j^{(n)} - \bar{Z}_j)/(N-1), \tag{22}$$

where

$$\bar{Z}_k \equiv \sum_{n=1}^{N} Z_k^{(n)}/N. \tag{23}$$

Finally, to enforce $\hat{\mathsf{C}}$ as being a *correlation* matrix, we use

$$\hat{\mathsf{C}}_{ij} \equiv \frac{\Sigma^*_{ij}}{\sqrt{\Sigma^*_{ii}}\sqrt{\Sigma^*_{jj}}}. \tag{24}$$

10 Estimation of grid-column averages

Let ψ be some scalar gridcolumn quantity that is ultimately definable in terms of gridcolumn temperature $\boldsymbol{T}$ and saturation ratio $\boldsymbol{S}$ and which therefore has a horizontal distribution within the grid-column. We define the gridcolumn mean (expectation value) of ψ as

$$\langle\psi\rangle \equiv \int_0^\infty \cdots \int_0^\infty \psi(\boldsymbol{t},\boldsymbol{s})\, p_{\boldsymbol{T},\boldsymbol{S}}(\boldsymbol{t},\boldsymbol{s})\, d\boldsymbol{t}\, d\boldsymbol{s}. \tag{25}$$

where $p_{\boldsymbol{T},\boldsymbol{S}}$ is the density of areal fraction within $(\boldsymbol{T},\boldsymbol{S})$ phase space, defined such that

$$F_{\boldsymbol{T},\boldsymbol{S}}(\boldsymbol{t},\boldsymbol{s}) = \int_0^{s_1} \cdots \int_0^{s_K} \int_0^{t_1} \cdots \int_0^{t_K} p_{\boldsymbol{T},\boldsymbol{S}}(\boldsymbol{t},\boldsymbol{s})\, d\boldsymbol{t}\, d\boldsymbol{s},$$

for all $\boldsymbol{t},\boldsymbol{s} \in [0,\infty]^K$. Note that this mean is a linear operator, namely $\langle a\psi\rangle = a\langle\psi\rangle$, and $\langle\psi+\phi\rangle = \langle\psi\rangle + \langle\phi\rangle$. Also, if ψ is only a function of a single layer T_k and S_k then the other layers are marginalized and we find

$$\langle\psi(T_k,S_k)\rangle = \int_0^\infty \int_0^\infty \psi(t,s)\, p_{T_k,S_k}(t,s)\, dt\, ds, \tag{26}$$

where $p_{T_k,S_k}(t,s) = \partial^2 F_{T_k,S_k}(t,s)/\partial t\, \partial s$.

For some ψ, such as the total or condensed water paths, the layer contributions appear linearly and so the $\langle\cdot\rangle$ passes through to individual layer evaluations in $\langle\psi\rangle$. This means that $\langle\psi\rangle$ can be evaluated as a weighted sum of single-layer marginal means as in (26). But for many other quantities, such as radiative transfer integrals, or surface precipitation flux, the ψ is a non-linear function of the layer contributions, and so $\langle\psi\rangle$ cannot be evaluated in terms of layer means, $\langle\cdot\rangle_k$. We will consider the numerical evaluation of such $\langle\psi\rangle$ in §11.

Finally, note that the expectation value $\langle\psi\rangle$ is invariant under any arbitrary transformation of $(\boldsymbol{T},\boldsymbol{S})$. In particular, for any one-to-one transformation to space $\boldsymbol{X} \subset \mathbb{R}^{2K}$ we may re-write (25) as

$$\langle\psi\rangle = \int_{\boldsymbol{X}} \psi(\boldsymbol{x})\, p_{\boldsymbol{X}}(\boldsymbol{x})\, d\boldsymbol{x}. \tag{27}$$

We may choose any transformation that is convenient for the evaluation of $\langle\psi\rangle$.

DOI: 10.1002/qj

11 Monte Carlo Subcolumn Generation

There are many quantities, such as the shortwave cloud transmittance, for which the integral in (25) or (27) does not have a simple analytic form and therefore requires evaluation by numerical methods. One such method involves the Monte Carlo generation of a finite number of "subcolumns" from the gridcolumn and then approximation of $\langle\cdot\rangle$ as the mean over this population of subcolumns. By a "subcolumn" we mean a description of all K layers at one particular horizontal location in the gridcolumn, as specified by a $2K$-vector $(\boldsymbol{T},\boldsymbol{S})$ or $\boldsymbol{X}$. The Monte Carlo subcolumn generator must produce a set of such subcolumns in a manner consistent with the underlying areal distribution function $F_{\boldsymbol{T},\boldsymbol{S}}$ (or $F_{\boldsymbol{X}}$) of the gridcolumn. While there exist other numerical methods that are more accurate, we will focus on Monte Carlo methods here because of the recent interest in Monte Carlo radiative transfer parameterizations for GCMs (e.g., Räisänen and Barker, 2004; Räisänen *et al.*, 2005).

11.1 A Gaussian Copula Subcolumn Generator

For the Gaussian copula, we may choose the monotonic increasing transformations $\boldsymbol{Z}$ in (12) so that

$$\langle\psi\rangle = \int_{\mathbb{R}^{2K}} \psi(\boldsymbol{z})\, p_{\boldsymbol{Z}}(\boldsymbol{z};\mathsf{C})\, d\boldsymbol{z}, \tag{28}$$

where $p_{\boldsymbol{Z}}(\boldsymbol{z};\mathsf{C})$ is defined by (13).

This suggests the following Monte Carlo method to estimate $\langle\psi\rangle$: (1) select N_S random sample vectors $\boldsymbol{Z}\in\mathbb{R}^{2K}$ from the distribution $N_{2K}(\boldsymbol{0},\mathsf{C})$, i.e., from a population with probability density $p_{\boldsymbol{Z}}(\boldsymbol{z};\mathsf{C})$, using Appendix B; (2) form a rank vector $\boldsymbol{R}$ for each $\boldsymbol{Z}$ using $R_k=\Phi(Z_k)$; (3) form a $\boldsymbol{T}$ and $\boldsymbol{S}$ for each $\boldsymbol{R}$ using the inverse of the marginal distributions, $T_k=F_{T_k}^{-1}(R_k)$ and $S_k=F_{S_k}^{-1}(R_{k+K})$, $k=1,\ldots,K$; (4) form a $\boldsymbol{q_c}$ for each $\boldsymbol{T}$ and $\boldsymbol{S}$ using $q_{ck}=(S_k-1)q_s(T_k)H(S_k-1)$ and any other intermediate quantities needed to evaluate a ψ for each sample; (5) finally, $\langle\psi\rangle_{N_S}^{\mathrm{GCOP}}$ is the mean of the N_S such ψ.

11.2 A Generalized Copula Subcolumn Generator

For any copula in general, one particular monotonic increasing transformation of $(\boldsymbol{T},\boldsymbol{S})$ is to rank space, namely,

$$\begin{aligned}(\boldsymbol{t},\boldsymbol{s})\mapsto\boldsymbol{r}\equiv(&F_{T_1}(t_1),\ldots,F_{T_K}(t_K),\\ &F_{S_1}(s_1),\ldots,F_{S_K}(s_K))^T.\end{aligned} \tag{29}$$

Evaluating $\langle\psi\rangle$ in this space,

$$\langle\psi\rangle = \int_{\boldsymbol{I}^{2K}} \psi(\boldsymbol{r})\,\frac{\partial^{2K}C_{\boldsymbol{T},\boldsymbol{S}}(\boldsymbol{r})}{\partial r_1\ldots\partial r_{2K}}\,d\boldsymbol{r}, \tag{30}$$

since the copula $C_{\boldsymbol{T},\boldsymbol{S}}$ is the areal distribution function in rank space. We may therefore use the following general Monte Carlo method to estimate $\langle\psi\rangle$: (a) select N_S random sample vectors $\boldsymbol{R}\in\boldsymbol{I}^{2K}$ from the copula $C_{\boldsymbol{T},\boldsymbol{S}}$, i.e., from a population with probability density function $\partial^{2K}C_{\boldsymbol{T},\boldsymbol{S}}(\boldsymbol{r})/(\partial r_1\ldots\partial r_{2K})$; (b) apply steps (3) and (4) from §11.1; (c) then $\langle\psi\rangle_{N_S}$ is the mean of the N_S such ψ.

The essense of this method is to generate random vectors in $\boldsymbol{I}^{2K}$ that are distributed according to a specified copula. Let us consider two particular cases of interest:

11.2.1 A "random overlap" copula

Based on the comments in §6.1, we model "random cloud overlap" using K independent layers and the product copula, $C_{\boldsymbol{S}}=\Pi^K$. To represent K independent layers, cloudy or not, while still retaining T and S correlations *within* each layer, we can use the copula

$$C_{\boldsymbol{T},\boldsymbol{S}}^{\mathrm{RAN}}(\boldsymbol{r}) = \Pi_{k=1}^{K} C_{T_k,S_k}(r_k,r_{k+K}), \tag{31}$$

where C_{T_k,S_k} is the marginal copula of layer k alone and $\boldsymbol{r}$ is the rank vector defined by (29). Note that, by (11) and the definition of a copula in §5, $C_{\boldsymbol{S}}^{\mathrm{RAN}}(v_1,\ldots,v_K)=\Pi_{k=1}^{K}C_{T_k,S_k}(1,v_k)=\Pi_{k=1}^{K}v_k$, as expected.

The intra-layer copula C_{T_k,S_k} can be a Gaussian copula or any other bivariate copula that is found to give a meaningful description of the rank dependence between T and S within the layer. We assume that we have a method of generating random temperature and saturation ratio rank pairs (R_k,R_{k+K}) from this copula. Such methods are described in Nelson (2006) and Appendix B of Sancetta (2005) and are also available as subroutines within MATLAB for example. For example, if we take $C_{T_k,S_k}(u,v)$ as the Gaussian copula $F_{\boldsymbol{Z}\in\mathbb{R}^2}(\Phi^{-1}(u),\Phi^{-1}(v);\mathsf{C}_k)$, where C_k is the correlation matrix for (Z_{Tk},Z_{Sk}) and $F_{\boldsymbol{Z}\in\mathbb{R}^2}$ is the two-dimensional ($K=1$) version of (15), then per §11.1 and our Appendix B, we may use $(R_k,R_{k+K})=(\Phi(G_1),\Phi(\rho_kG_1+\sqrt{1-\rho_k^2}G_2))$, where ρ_k is the correlation coefficient of Z_{Tk} and Z_{Sk}, i.e., the off-diagonal element of C_k, and where G_1,G_2 are independently distributed $\sim N(0,1)$. Finally, the independence between layers is achieved in the Monte Carlo process by doing this single layer generation independently for each layer.

11.2.2 A "maximum overlap" copula

The generation of maximum overlap is not trivial for the case where the intra-layer correlation of T and S is to be preserved. We present a method in Appendix C for generation of maximally overlapped saturation S and therefore maximally overlapped clouds for the case in which each intra-layer copula is Gaussian.

12 Some Preliminary Tests

This paper is mainly intended as a theoretical outline of our new approach to dealing with cloud overlap. We will show here only some preliminary numerical results using synthetic data from a cloud resolving model simulation and present a more extensive testing in a follow-up paper.

DOI: 10.1002/qj

12.1 Goddard Cumulus Ensemble Model

We use output from a Goddard Cumulus Ensemble (GCE) model simulation of the Atmospheric Radiation Measurement (ARM) Spring 2000 Intensive Operation Period (IOP) over the Southern Great Plains (SGP) site. The simulation has 128×128 gridpoints per layer with a 1km grid spacing, and 41 levels in the vertical, spread non-uniformly from the surface through 22km. The GCE model is non-hydrostatic with a bulk microphysics scheme including three species of ice: crystals, snow and graupel. Details of the model and an analysis of this particular simulation can be found in Zeng *et al.* (2007).

12.2 A preliminary 12-layer test

We consider the overlap of the GCE model's lowest twelve layers from a single snaphot of the GCE simulation output at 1831Z on 16 March 2000, about 15 days into a 20 day simulation, and about one day after the passage of a cold front through the domain. The lowest 12 layers are precisely the ones that contain no gridpoints with $T < 0°$C and no cloud ice in this snapshot. Each of these layers contains 128×128 gridpoints, and the twelve layers together form a simplified "grid-column" for the cloud fraction tests to follow. The mean profile of temperature for these layers, which extend from the surface to about 2km, is shown in Figure 1a.

For each gridbox in our simplified gridcolumn, we form a total water content q_t by summing the model vapor and condensed (but non-precipitating) cloud water contents. The mean profile of q_t is shown in Figure 1b and together with the temperature profile shows a relatively warmer, moister airmass overlying a poorly mixed surface layer up to 800m. The upper airmass is the air that has been lifted by the passing coldfront, and the lower layer is the colder, drier air that swept under it. The bulk condensed water content, q_c and saturation ratio, S, are then calculated according to assumption (A4), §3. Figure 1c shows the presence of some condensed water in each of the twelve layers.

Figure 2 shows horizontal slices of T and q_c for the GCE snapshot for three selected layers: 3, 5, and 12, with mid-layer heights at 214, 470, and 2122 meters above the surface. Layer 3 has a complex structure containing narrow, string like perturbations with high T and q_c (shown) and also high q_t and strong upward motion (not shown). These are cumulus cloud bands associated with surface-driven warm, moist convective updrafts. These form readily in the lower region because the surface has been recently wet by frontal rain and the latent heat flux is high. Layer 12, conversely, is representative of the warmer, moister, frontally raised airmass and is characterized by a much more slowly varying, large scale cloud field surrounding a distinct clear region. Finally, layer 5, is in the transition between these two airmasses and shows elements of both.

We will estimate a Gaussian copula using the T and S data from this twelve layer snapshot, as described below, and then see how our copula-based cloud fraction and column radiative properties compare with the exact snapshot properties and with the properties predicted by other methods applied to this synthetic grid-column.

12.2.1 Cloud Fraction

We define the "true" cloud fraction for each layer f_k^{true} as the fraction of gridboxes per layer which have $S > 1$. These are shown as the solid line in Figure 1d. Notice again that there is cloud in every layer, even though we have inferred from the the temperature and moisture profiles above that we are likely looking at two different air masses. This observation gives further reason why a "maximum overlap" assumption should not automatically be applied to a vertically contiguous set of cloudy layers.

The true *column* cloud fraction f^{true} is 0.9321. This is the fraction of the 128×128 horizontal points for which at least one layer has some condensate. By comparison, the column cloud fractions formed by the random overlap and maximum overlap assumptions, using the f_k^{true} as input, are 1.0000 and 0.7157, respectively. We will call these $f_{\text{RAN}}^{(\text{true})}$ and $f_{\text{MAX}}^{(\text{true})}$. They are in error by 7.3% and -23.2% respectively (see also Table I). Again, while neither random or maximum overlap is realistic, in this case maximum overlap is very unrealistic, even though the whole layer is "contiguously cloudy" in the vertical.

Next we fit an appropriate marginal distribution function to each layer's T and S data. Various distributions were tried, but the Generalized Extreme Value[8] (GEV) Distribution proved to give the best fits. The maximum likelihood fits are shown in the top panels of Figures 3 and 4 for the same three selected layers shown in Figure 2. The layer 3 and 5 fits are generally very good, although the narrow localized peak at $S = 1$ is not captured for layer 3. The layer 12 fits are poorer — it seems that although the GEV distribution is generally reasonable, it cannot model a broad distribution with an additional sharp peak. Future work should be done to select an improved marginal distribution, possibly one that is the sum of two distributions, one to handle the main spread, and another to model an additional peak. Finally, note how both positively and negatively skewed marginal distributions are needed for T_k and S_k. The marginals are clearly non-Gaussian.

From the GEV best fit margins, which we denote by $F_{T_k}^{\text{GEV}}$ and $F_{S_k}^{\text{GEV}}$, we evaluate the "fitted" layer cloud fractions as follows: $f_k^{\text{fit}} = 1 - F_{S_k}^{\text{GEV}}(1)$ using (3). These f_k^{fit} values are shown as the dashed line in Figure 1d. In the

[8]The Generalized Extreme Value distribution is defined by

$$F_X(x; \mu, \sigma, \xi) = \exp\left\{ -\left[1 + \xi\left(\frac{x-\mu}{\sigma}\right)\right]^{-1/\xi} \right\}$$

for $1 + \xi(x - \mu)/\sigma > 0$, where $\mu \in \mathbb{R}$ is the location parameter, $\sigma > 0$ is the scale parameter and $\xi \in \mathbb{R}$ is the shape parameter. It can handle both positively and negatively skewed distributions as Figures 3 and 4 show. For $\xi > 0$, the distribution is bounded below, and has an infinite tail in the positive x direction. Conversely for $\xi < 0$, the distribution is bounded above, and has an infinite tail in the negative x direction. However, for the distributions of positive q_t we are studying, there will, in practice, be negligible probability for $q_t < 0$.

DOI: 10.1002/qj

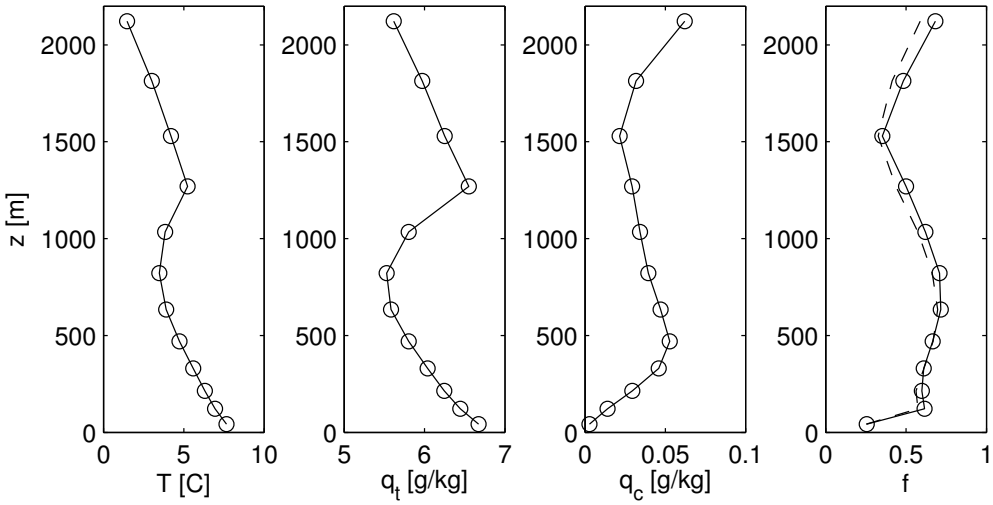

Figure 1. (a)-(c) Layer mean profiles for the lowest twelve layers of the GCE snapshot (see text) of temperature, T, total water content, q_t, and condensed water content, q_c; (d) The $f_k^{\rm true}$ (solid) and $f_k^{\rm fit}$ (dashed) layer cloud fractions (see text).

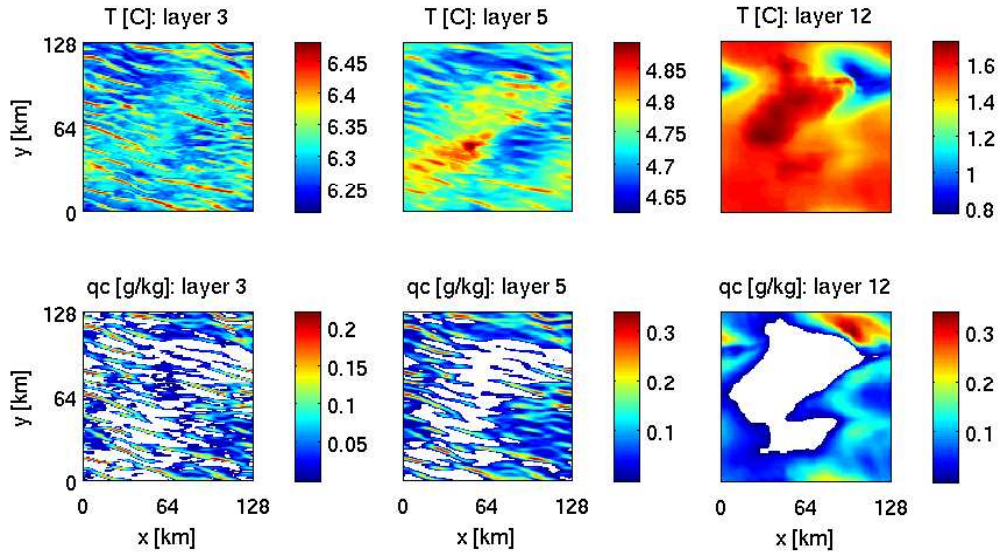

Figure 2. Horizontal slices of the GCE snapshot at layers 3, 5 and 12, for temperature (top) and condensed water content (bottom).

upper airmass, especially, these $f_k^{\rm fit}$ tend to underestimate $f_k^{\rm true}$ by 10–15%. For layer 12 shown in Figure 4 we can see that this underestimate stems from failing to capture the sharp peak in S just above $S = 1$. The random and maximum overlap column fractions calculated using the $f_k^{\rm fit}$ are as follows: $f_{\rm RAN}^{\rm (fit)} = 0.9999$ and $f_{\rm MAX}^{\rm (fit)} = 0.6963$, which are in error by 7.3% and -25.3% of $f^{\rm true}$.

Next, sample ranks are assigned using (21) with the GEV marginal distributions just described, and these are then transformed to Z_k space using (12) and (18). The binned PDFs of the Z_{Tk} and Z_{Sk} are shown in the lower panels of Figures 3 and 4. As expected, the distributions of the Z_k are close to $N(0, 1)$, at least for layers 3 and 5. Then, as per §9, we approximate the correlation matrix $\hat{\rm C}$ from the $Z_k^{(n)}$ using (24) and (22). At this point the Gaussian copula (20) is fully specified, and we can evaluate the column cloud fraction via (6). This evaluation can use either the $f_k^{\rm true}$ or $f_k^{\rm fit}$, yielding the following two Gaussian copula estimates of the column cloud fraction: $f_{\rm GCOP}^{\rm (true)} = 0.9096$ and $f_{\rm GCOP}^{\rm (fit)} = 0.8835$. These are in error by -2.4% and -5.2% of $f^{\rm true}$. These errors are less than the respective errors associated with the random or maximum overlap column cloud fractions (see Table I) and demonstrate, at least for this simple test case, the utility of the Gaussian copula cloud fraction method.

Since both $f_{\rm GCOP}^{\rm (true)}$ and $f_{\rm GCOP}^{\rm (fit)}$ depend on the GEV fits, via the assignment of the sample ranks used to calculate the Z_k, it seems likely that an improved marginal model (such as the sum of two distributions, as suggested earlier) would further improve the Gaussian copula results. Finally, note that we could have alternatively assigned empirical ranks to the T_k and S_k data, without fitting any model distribution, just by using the position of gridpoint values within a sorted list for each layer. We decided to

DOI: 10.1002/qj

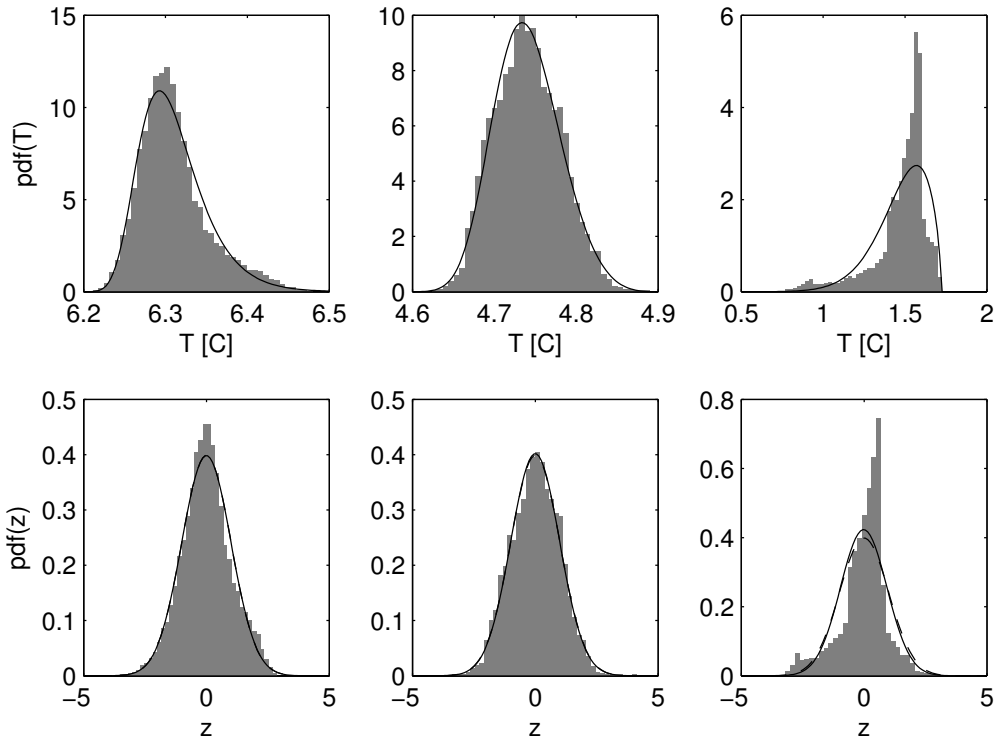

Figure 3. Top: the binned frequency distribution of T_k data for layers 3, 5 and 12 expressed in probability density units (shaded gray) and the probability density function (solid line) corresponding to the maximum likelihood fit of the Generalized Extreme Value (GEV) Distribution to the T_k data. Bottom: the corresponding frequency distributions of Z transformed from T_k using (12) and (18) in gray, and the probability density of a maximum likelihood fit of a normal distribution as the solid line. The standard normal probability density function $N(0,1)$ is plotted as a dashed line for comparison, but it is only distinguishable from the maximum likelihood fit in layer 12, and then only slightly.

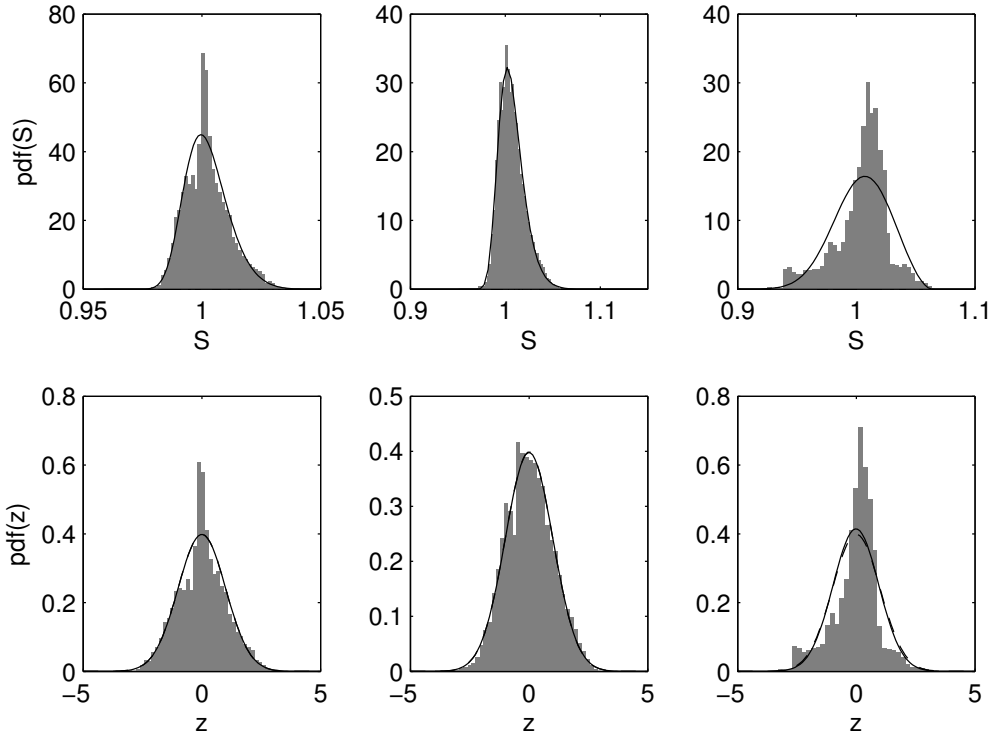

Figure 4. As for Figure 3 but for the distributions of saturation ratio, S_k. Left to right are layers 3, 5 and 12.

DOI: 10.1002/qj

Table I. Column cloud fractions (and their % bias with respect to the GCE reference $f^{\text{true}} = 0.9321$) for methods χ = GCOP, MAX and RAN. The $f_\chi^{(\text{true})}$ row uses the actual GCE layer cloud fractions, f_k^{true}, while the $f_\chi^{(\text{fit})}$ row uses the $F_{S_k}^{\text{GEV}}$-derived layer fractions, f_k^{fit}.

	GCOP	MAX	RAN
$f_\chi^{(\text{true})}$	0.9096 (-2.4%)	0.7157 (-23.2%)	1.0000 (7.3%)
$f_\chi^{(\text{fit})}$	0.8835 (-5.2%)	0.6963 (-25.3%)	0.9999 (7.3%)

use the marginal fitting approach instead, since our ultimate plan is to use the new copula method in tandem with PDF-based cloud parameterizations within GCMs, in which case a parameterized marginal distribution function is needed.

12.2.2 Radiative Transfer

Though we first conceived the use of copulas as a means of approximating column cloud fraction, we have shown in §10 and §11 that copula methods can also be used to generate ensembles of "subcolumns," consistent with an underlying distribution, over which gridcolumn means of non-linear radiative properties may be approximately evaluated.

Consider some radiative quantity, ψ, for which we want to estimate the gridcolumn average $\langle\psi\rangle$. Our reference calculation $\langle\psi\rangle_{\text{ICA}}^{\text{GCE}}$ is the Independent Column Approximation (ICA) calculation in which ψ is evaluated for each of the 128×128 or 16384 subcolumns comprising the GCE snapshot and the results averaged. Next, to study the effect of subsampling these GCE subcolumns, we evaluate $\langle\psi\rangle_{N_S}^{\text{GCE}}$, the average of ψ over N_S randomly selected subcolumns from the GCE snapshot, with $N_s = 2^n, n = 1, \ldots, 10$. For each such N_S we do 1000 independent evaluations of $\langle\psi\rangle_{N_S}^{\text{GCE}}$ to characterize the spread in $\langle\psi\rangle_{N_S}^{\text{GCE}}$ arising from the stochastic nature of the random subcolumn selection (see below).

We also evaluate an "eXact Overlap Randomized" result, $\langle\psi\rangle_{N_S}^{\text{XOR}}$, in the same way as we evaluate $\langle\psi\rangle_{N_S}^{\text{GCE}}$, using an exact copy of the 16384 GCE subcolumns, except that, layer by layer, we randomly rearrange the positions of cloudy gridpoints, while leaving the clear gridpoints untouched. This preserves exactly the geometrical cloud overlap found in the GCE subcolumns, and also preserves the joint distribution of T and S within each layer, but destroys the vertical correlations of in-cloud properties between layers[9]. The XOR method can thus been seen as a way of isolating the effects of geometrical cloud overlap from the effects of vertical correlation of in-cloud properties such as T and q_c.

[9]The XOR method is similar to another method, which we call "eXact Overlap Homogenized" or XOH, in which the GCE subcolumns are kept unchanged, except for homogenizing the q_c values in the cloudy gridpoints of each layer. We find that the biases of the XOH results are similar to, but slightly larger (in an absolute sense) than the biases for XOR, for each of the ψ we later consider. Thus we will not include the XOH results in our following analysis.

Finally, we also generate three copula results, $\langle\psi\rangle_{N_S}^{\text{GCOP}}$, $\langle\psi\rangle_{N_S}^{\text{RAN}}$, and $\langle\psi\rangle_{N_S}^{\text{MAX}}$, using the Gaussian, random, and maximum copula generators described in §11.1, §11.2.1, and §11.2.2. The Gaussian copula generator (GCOP) uses the 24×24 sample correlation matrix $\hat{\mathsf{C}}$ of the 16384 $\boldsymbol{Z}^{(n)} \in \mathbb{R}^{24}$ as per §9. In contrast, the random and maximum copula generators use a separate Gaussian copula for each of the 12 layers, characterized by $\hat{\mathsf{C}}_k$, the 2×2 sample correlation matrix of the 16384 $(Z_{Tk}^{(n)}, Z_{Sk}^{(n)}) \in \mathbb{R}^2$.

In order to preserve an identical sampling stategy among all the $\langle\psi\rangle_{N_S}$ variants, we generate a pool of exactly 16384 subcolumns from each of the three copula generators, and then select 1000 lots of N_S subcolumns from this pool, for each N_S, i.e., the same sampling strategy as for $\langle\psi\rangle_{N_S}^{\text{GCE}}$ and $\langle\psi\rangle_{N_S}^{\text{XOR}}$. We note that for $N_S = 1024$, for example, we will be selecting 1000 lots of 1024 random subcolumns each, from a total of only 16384 available subcolumns, so the spread of $\langle\psi\rangle_{N_S}$ for high N_S values will be artificially reduced by multiple reselection of the same subcolumns. We are not particularly concerned about this, first because the spread will already be small for large N_S, but more importantly, because this reduction in spread applies equally to each type of $\langle\psi\rangle_{N_S}$. We are concerned primarily with the relative biases of the different methods, not in a precise evaluation of the spread in $\langle\psi\rangle_{N_S}$ at high N_S.

The preceeding paragraphs define the sampled gridcolumn means $\langle\psi\rangle_{N_S}^{\chi}$ for χ = GCE, GCOP, XOR, MAX, and RAN, as well as the reference $\langle\psi\rangle_{\text{ICA}}^{\text{GCE}}$ mean over all 16384 subcolumns of the GCE snapshot. We also define the additional ICA means $\langle\psi\rangle_{\text{ICA}}^{\chi}$, for χ = GCOP, XOR, MAX, and RAN, as the mean ψ over all 16384 subcolumns produced for method χ. Also, in all that follows, when we refer to the percentage bias or just "bias" in $\langle\psi\rangle_{N_S}^{\chi}$ or $\langle\psi\rangle_{\text{ICA}}^{\chi}$ we mean its percentage error with respect to the $\langle\psi\rangle_{\text{ICA}}^{\text{GCE}}$ reference.

We will study the shortwave (SW) transmittance, TRN, and reflectance, RFL, [i.e., the downwelling SW flux at the surface and the upwelling SW flux at the top of the atmosphere (TOA), both normalized by the downwelling SW flux at the TOA] and the downwelling longwave (LW) flux at the surface, DLR, and outgoing LW flux at TOA, OLR, as evaluated by the SW (Chou *et al.*, 1998; Chou and Suarez, 1999) and LW (Chou *et al.*, 2001) column radiation models used in various NASA-GSFC Large Scale models[10]. The surface was assumed black for both SW and LW calculations (i.e, zero surface albedo and unit emissivity across the spectrum) with a temperature of 281.73 K from the GCE. The temperature and water vapor profile used above the lowest 12 layers comes from the mean GCE fields up to a pressure of 37 mb (the top of the GCE domain) and from a standard mid-latitude summer (MLS) profile above that level. The profile of ozone molecular concentrations also comes

[10]Clearly the overlap assumptions of these column radiation codes are turned off, since they are being applied iteratively to single subcolumns for which each layer is either overcast or clear.

DOI: 10.1002/qj

Table II. Percentage biases in gridcolumn means $\langle\psi\rangle^{\chi}_{\rm ICA}$ for χ = GCOP, XOR, MAX, and RAN, with respect to reference $\langle\psi\rangle^{\rm GCE}_{\rm ICA}$.

ψ	$\langle\psi\rangle^{\rm GCE}_{\rm ICA}$	GCOP	XOR	MAX	RAN
TRN	0.4768	0.15	-10.83	8.44	-22.09
RFL	0.3158	-0.14	14.13	-10.85	28.74
DLR	334.36 W/m^2	-0.22	1.47	-3.18	4.10
OLR	236.68 W/m^2	0.17	-0.18	0.45	-0.49

from the same MLS profile, while the CO_2 concentration was set to 370 ppm throughout the domain. The solar code used an overhead sun. An effective radius for cloud droplets of 10 microns was assumed.

Table II shows the $\langle\psi\rangle^{\rm GCE}_{\rm ICA}$ reference means for our 12-layer test case, together with the corresponding biases in the other ICA means ($\langle\psi\rangle^{\chi}_{\rm ICA}$ for χ = GCOP, XOR, MAX, and RAN). For the SW quantities TRN and DLR, the GCOP biases are *much* smaller than for the other methods and strongly support the utility of the GCOP method, which nicely models the effects of both geometrical cloud overlap and vertical correlation of in-cloud properties.

The signs of the the other SW biases can be explained as follows: (XOR) Note that randomizing each layer's cloudy gridpoints does *not* homogenize the cloud on a layer by layer basis, since we ignore all non-plane-parallel effects in our radiative transfer calculations, but it *does* tend to homogenize vertically integrated cloud properties, such as the condensed water path, in regions where multiple GCE cloud layers contribute. This explains the signs of the SW biases for XOR, which are consistent with the so-called "plane parallel bias" in which homogenizing the condensed water path in a cloud makes it less transmissive and more reflective in the SW, due to the non-linear dependence of cloud albedo on optical depth; (MAX) Maximum cloud overlap produces the maximum column clear fraction and therefore promotes transmittance over reflectance. Furthermore, the maximum generator we have employed produces highly inhomogeneous cloud water paths, in the sense that saturation ratio is maximally rank correlated in the vertical. This produces the opposite of the plane-parallel bias just described, yielding larger cloudy transmittance and smaller reflectance; (RAN) Random overlap underestimates column clear fraction and therefore transmittance. It also has a homogenizing effect on the condensed water path, as described under XOR, and therefore also underestimates transmittance due to the plane-parallel bias previously described.

The following conclusions (for this test case) can be drawn from the sizes of the SW biases: (1) It is very important to consider the vertical correlation of in-cloud quantities, not just the correct geometrical cloud overlap, since even with exact overlap, the XOR SW biases exceed 10%. Compare this with the very small biases for GCOP — evidently the correct modeling of inter-layer correlations of in-cloud properties by GCOP, which XOR destroys, more than compensates for its non-exact column cloud fraction. (2) The accuracy of prediction of the column cloud fraction is a poor indicator of the quality of the solar transmittance and reflectance. First, as above, a perfect column cloud fraction in XOR still yields in excess of 10% biases in TRN and RFL. Second, as per Table I, the RAN cloud fraction only has a 7% error but SW biases in excess of 20% while the MAX cloud fraction is in error by more than 20% but has significantly smaller SW biases, about one third those of RAN. Judging from the cloud fraction alone it appears that RAN is better than MAX, but the exact reverse is true for TRN and RFL. This value judgment about f comes as no surprise really: there is broad awareness in the GCM parameterization community that the cloud fraction is a rather imprecise quantity, especially as it relates to radiative transfer — a thin cloud may have negligible radiative effect even though being technically classified as cloud.

Next consider the LW biases for DLR and OLR. Again, GCOP gives the smallest biases, but the results are not nearly as definitive as for SW, and especially for OLR, which is never in error by more that 0.5%. The analysis of the LW biases is complicated (c.f. SW) by the importance of temperature variability, but we make the following observations: (1) The exact cloud fraction (XOR) biases are smaller than for MAX and RAN, indicating that the accuracy of the cloud fraction f is more important in the LW than in the SW. This is consistent with the fact that clouds become black in the LW faster than they become saturated in SW reflectance, and so thinner clouds, which contribute as much to f as thicker clouds, become more important; (2) The larger biases for DLR compared to OLR can be explained by the greater contrast between the brightness temperatures of the clouds and the clear sky than between the clouds and the surface; (3) The signs of the XOR, MAX, and RAN biases are consistent with the LW version of the "plane-parallel bias", namely that the homogenization of cloud water path causes an increase in emissivity, due to the non-linear dependence of emissivity on cloud water path. Thus the XOR and RAN methods, which tend to homogenize cloud water path, act to blacken the clouds and therefore cause them to radiate at an effective emitting height closer to the boundary of the cloud. For DLR this causes the LW radiation to come from closer to the cloud base, which is a warmer region due to the temperature lapse rate (see Figure 1a). Conversely, homogenization produces an effective emitting height closer to the top of the cloud for OLR, which is generally a cooler region. This is consistent with the signs of the LW biases for XOR and RAN in Table II. The signs of the MAX biases are just the opposite, since the MAX method tends to increase cloud inhomogeneity, as described above for SW. (4) The signs of the LW biases for MAX and RAN are also consistent with a simple column cloud fraction effect: RAN overestimates column cloud fraction and thereby shields the cold sky for DLR and warm surface for OLR, thus contributing to positive and negative biases in DLR and OLR, respectively. The opposite is true for MAX which underestimates column cloud fraction.

DOI: 10.1002/qj

Clearly, both the cloud fraction and cloud homogenization biases are in operation together for MAX and RAN, while the XOR method retains only the homogenization bias. Finally, note that these LW biases are consistent with the results presented by Li and Barker (2002).

We have noted that although GCOP is still the best performer in the LW, its relative improvement over MAX, RAN or XOR is less than for the SW. We believe that this is in part due to the importance of temperature variability in the LW, and the fact that the fitting of the marginal temperature distributions could be improved, especially for the upper cloud in this test case (e.g., Figure 3, top right panel). It is our hope that the LW GCOP results will further improve with an improved marginal model, such as the two-component marginal proposed in §12.2.1.

Figures 5 and 6 summarize the biases of sampled means $\langle\psi\rangle^{\chi}_{N_S}$ (χ = GCE, GCOP, XOR, MAX, and RAN) with respect to the reference $\langle\psi\rangle^{\mathrm{GCE}}_{\mathrm{ICA}}$ values. The vertical lines show the observed spread of $\langle\psi\rangle^{\chi}_{N_S}$ bias over the 1000 iterations in the 25%–75% and 2.5%–97.5% percentile ranges. The horizontal lines show the biases in the $\langle\psi\rangle^{\chi}_{\mathrm{ICA}}$, as per Table II. We make the following observations: (1) The statistical spread in each $\langle\psi\rangle^{\chi}_{N_S}$ decreases as the number of subcolumn samples is increased; (2) The middle half (inter-quartile range) of the spread of the $\langle\psi\rangle^{\mathrm{GCOP}}_{N_S}$ has an absolute error smaller than the bias for $\langle\psi\rangle^{\mathrm{XOR}}_{\mathrm{ICA}}$ for $N_S \geq 16$ for TRN, RFL, and DLR. This means that the majority of sampled $\langle\psi\rangle^{\mathrm{GCOP}}_{N_S}$ estimates will beat the XOR ICA calculation for as few as 16 sampled subcolumns. The OLR biases are already very small and can be estimated to within about 1% by any method the majority of the time for $N_S \geq 16$.

13 Conclusions and Potential Applications

We have shown that a general representation of GCM column cloud fraction within the PDF-based statistical cloud parameterization context can be obtained by the use of statistical functions called "copulas" that encapsulate the dependence structure of rank statistics in a multivariate system. Using this theory and cloud resolving model (CRM) simulations for guidance, a new formulation of GCM cloud overlap has been obtained.

We find that Gaussian copula estimates of column cloud fraction for a 12-layer test case using synthetic data from a Goddard Cumulus Ensemble simulation are an improvement over both random and maximum overlap estimates. Furthermore, Gaussian copula Monte-Carlo estimates of the non-linear SW transmittance and reflectance and the LW surface downwelling and TOA outgoing radiation showed very significant improvement over the maximum or random generators for this test case. The Gaussian copula generator method also outperforms the exact overlap randomized (XOR) method described in the text. In fact, for a majority of the Monte-Carlo results, the absolute bias calculated over as few as 16 randomly selected subcolumns from the Gaussian copula generator, is less than the bias for an infinite number of XOR subcolumns. These results suggest significant potential for the copula-based parameterization of cloud overlap in future GCM cloud radiation parameterizations. In a follow-up paper, we will present a more extensive testing of the method using GCE simulations for a range of synoptic conditions.

This paper has concentrated on the general theory of the application of copulas to the description of the horizontal and vertical distribution of temperature and water content within a GCM-like gridcolumn. We provide this theoretical basis in the hope that it will be used to develop a new set of GCM cloud parameterizations. Our initial thoughts on how this might be done are as follows: (1) Our starting point is that a good GCM parameterization should be governed by a reasonably small number of parameters which are prognosticated or diagnosed. The method described in this paper requires a small set of marginal distribution parameters for F_{T_k} and F_{S_k} for each of the K model layers, and a $2K \times 2K$ correlation matrix describing the Gaussian copula of $\boldsymbol{T}$ and $\boldsymbol{S}$. The $K(2K-1)$ unique elements of this correlation matrix C are excessive for the purposes of parameterization, so we will seek an appropriate model of C with one or several length scale parameters, following the work of Gaspari and Cohn (1999) and Gaspari *et al.* (2006); (2) The GEV distributions used for F_{T_k} and F_{S_k} each have three parameters (a location, scale, and shape parameter) which are roughly equivalent to the specification of the mean, variance, and skewness for each of temperature and saturation ratio. These will be prognosticated following the lead of Tompkins (2002). A suitable diagnostic or prognostic parameterization for the correlation length scales used to model C will also be needed; (3) The marginal-estimated layer cloud fractions and the copula-estimated column cloud fraction can be output as diagnostics. The radiative transfer calculations will use the Gaussian copula generator (§11.1) as an alternative to the more empirical generator of Räisänen *et al.* (2004) in the implementation of the Monte Carlo ICA method of Räisänen and Barker (2004).

We also envisage the usefulness of such a copula-based GCM cloud parameterization within the context of data assimilation for NWP applications. The high horizontal and vertical resolution cloud data available from current satellites (e.g., from MODIS on EOS Terra and Aqua, and from CloudSat and other A-Train satellites) and anticipated from future satellite missions (e.g., NPOESS) holds a wealth of statistical information on the distribution of cloud water inside GCM-sized gridcolumns. We envisage the use of this cloud data to update the marginal and copula parameters of the new GCM parameterization using a parameter estimation approach (e.g., Norris and da Silva, 2007; Dee and da Silva, 1999; Dee *et al.*, 1999). In this way the information from high-resolution satellite observations can be incorporated into global analyses.

Acknowledgements

This work was partially supported by the NASA Interdisciplinary Science Program at Goddard Space Flight

DOI: 10.1002/qj

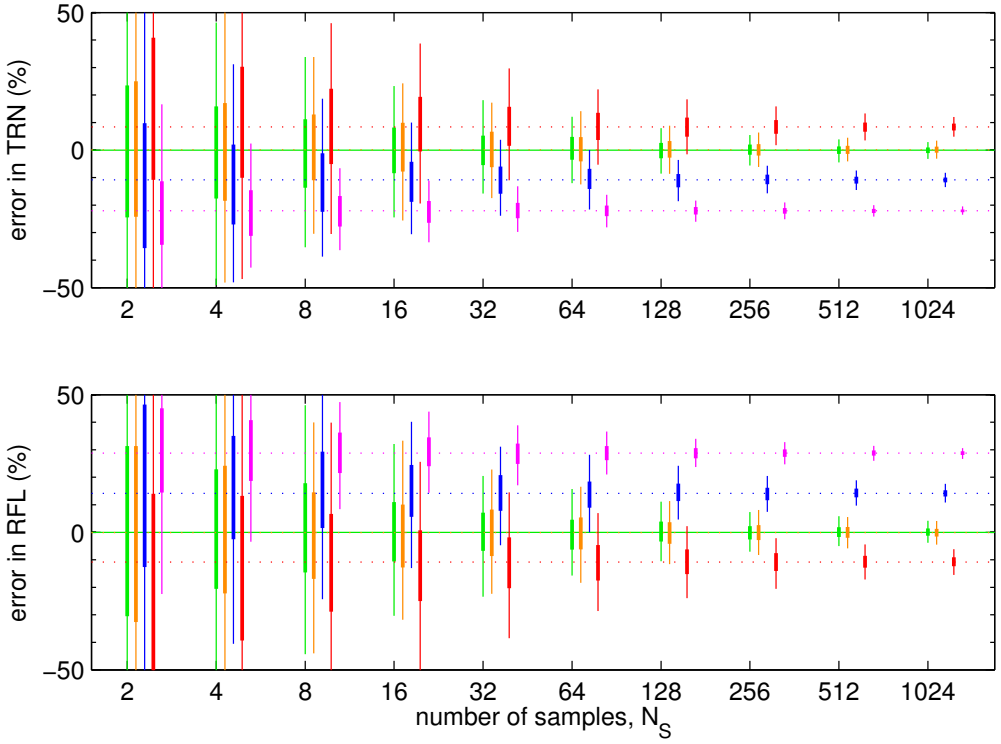

Figure 5. Errors in $\langle\psi\rangle^{\chi}_{N_S}$ w.r.t. the $\langle\psi\rangle^{\mathrm{GCE}}_{\mathrm{ICA}}$ reference for the shortwave transmittance and reflectance, $\psi = TRN$ and RFL, and $N_S = 2, 4, \ldots, 1024$. Each N_S group shows five methods, from left to right: χ = GCE (green), GCOP (orange), XOR (blue), MAX (red), and RAN (magenta). The horizontal offset within each group is for viewing ease only. The thick vertical lines show the inter-quartile range among 1000 independent evaluations. The thin vertical lines are the 2.5%–97.5% percentile ranges. The horizontal lines show the biases in $\langle\psi\rangle^{\chi}_{\mathrm{ICA}}$, i.e., the error in the mean ψ over all 16384 χ-generated subcolumns, as per Table II.

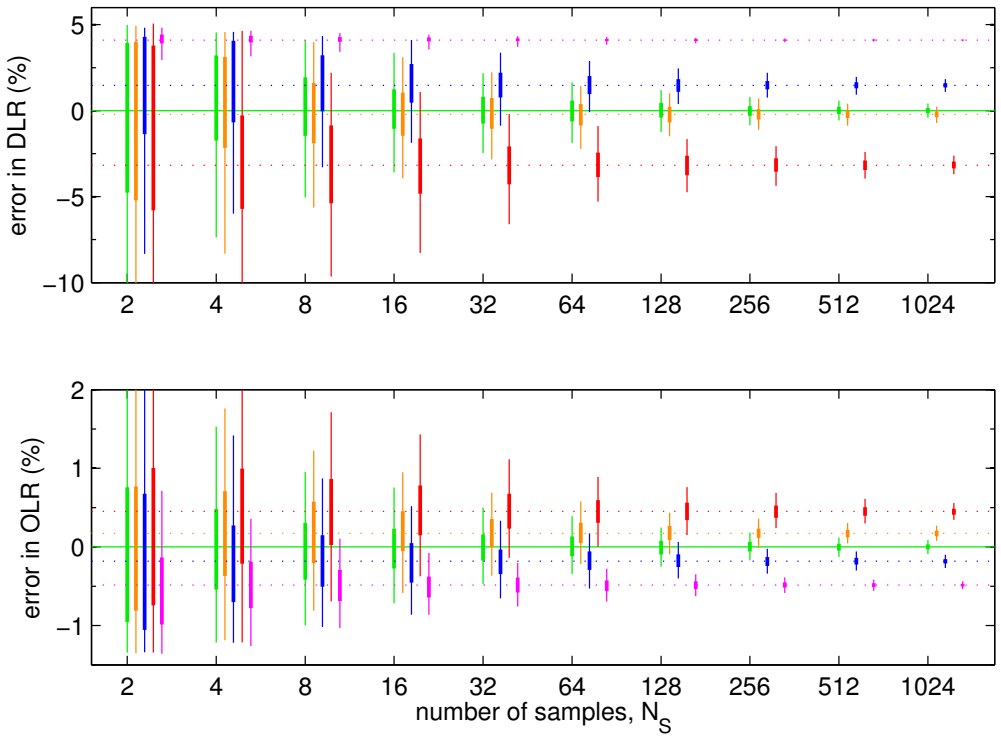

Figure 6. As for Figure 5, but for the longwave quantities $\psi = DLR$ and OLR, the downwelling flux at the surface and outgoing flux at TOA, respectively.

DOI: 10.1002/qj

Center under WBS-51-291-01-C7. Lazaros Oreopoulos greatfully acknowledges support for this work by the US Department of Energy, Office of Science, Office of Biological and Environmental Research, Environmental Sciences Division as part of the ARM program under grant DE-FG02-07ER64354. The authors wish to thank Drs. Stephen Cohn and Julio Bacmeister and Mr. Stephen Lang for useful discussions.

A Copulas for multiple cloud layers

One commonly applied assumption is that vertically separated cloud blocks (i.e., vertically contiguous blocks of at least partially cloudy model layers, separated by completely clear model layers) are randomly overlapped. We shall call this the "Random Overlap Across Clear Layers" or ROACL assumption. Say there are M such blocks of cloud, defined by

$$\{f_1'^{(1)},\ldots,f_{K^{(1)}}'^{(1)}\},\ldots,\{f_1'^{(M)},\ldots,f_{K^{(M)}}'^{(M)}\},$$

such that all of the included model layers are at least partially cloudy (i.e., all $f_k'^{(j)}<1$). The column clear fraction for block (j) is

$$f'^{(j)}=C_{\boldsymbol{S}}^{(j)}(f_1'^{(j)},\ldots,f_{K^{(j)}}'^{(j)}),$$

where $C_{\boldsymbol{S}}^{(j)}$ is the marginal copula for block (j) layers only. Then, since the blocks are randomly overlapped, the clear fraction for the entire column is given by

$$f'_{\text{ROACL}}=\Pi_{j=1}^{M}C_{\boldsymbol{S}}^{(j)}(f_1'^{(j)},\ldots,f_{K^{(j)}}'^{(j)}).$$

One common subset of ROACL are the maximum-random overlap schemes. The Tian and Curry (1989) version, which we will denote MRO, specifies maximum cloud overlap within blocks, and so has

$$f'_{\text{MRO}}=\Pi_{j=1}^{M}\min(f_1'^{(j)},\ldots,f_{K^{(j)}}'^{(j)}).$$

B Multinormal Random Number Generation

A multinormal random vector $\boldsymbol{Z}=(Z_1,\ldots,Z_{2K})^T\sim N_{2K}(\boldsymbol{0},\mathsf{C})$, where C is a strictly positive definite correlation matrix, can be generated as follows: $\boldsymbol{Z}=\mathsf{H}\boldsymbol{G}$ where H is the lower-triangular Cholesky decomposition of C, such that $\mathsf{C}=\mathsf{H}\mathsf{H}^T$ and H has strictly positive diagonal entries, and $\boldsymbol{G}=(G_1,\ldots,G_{2K})^T$ is a vector of independent standard normal variates, i.e., each $G_k\sim N(0,1)$ independently.

For the two dimensional case ($K=1$),

$$\mathsf{C}=\begin{pmatrix}1&\rho\\ \rho&1\end{pmatrix}\quad\text{and}\quad\mathsf{H}=\begin{pmatrix}1&0\\ \rho&\sqrt{1-\rho^2}\end{pmatrix},\qquad(32)$$

where $\rho\in(-1,1)$ is the correlation coefficient, and $\boldsymbol{Z}=(G_1,\rho G_1+\sqrt{1-\rho^2}G_2)^T$ has a particularly simple form.

C Maximum Overlap Generator

In §6.1.2 we noted that "maximum cloud overlap" in K layers can be represented by the "M-copula", i.e., using $C_{\boldsymbol{S}}(r_1,\ldots,r_K)=\min(r_1,\ldots,r_K)$. The areal density in rank space is therefore zero off the the main diagonal of $\boldsymbol{I}^K$, suggesting that a simulation scheme for the ranks should use the same uniform rank for each dimension. Namely if we select random rank vectors $\boldsymbol{R}\equiv(U,\ldots,U)^T\in\boldsymbol{I}^K$, where U is uniformly distributed on $[0,1]$, then for infinite samples,

$$\begin{aligned}\text{Fr}(R_1\le r_1,\ldots,R_K\le r_K)&=\text{Fr}(U\le r_1,\ldots,U\le r_K)\\&=\text{Fr}(U\le\min(r_1,\ldots,r_K))=\min(r_1,\ldots,r_K),\end{aligned}$$

as required. It is clear, then, that the M-copula gives the maximum possible correlation between all the K ranks.

The definition of "maximum overlap" in the $2K$ space $(\boldsymbol{T},\boldsymbol{S})$ is not as trivial. We still want

$$\begin{aligned}C_{\boldsymbol{S}}(r_1,\ldots,r_K)&=C_{\boldsymbol{T},\boldsymbol{S}}(1,\ldots,1,r_1,\ldots,r_K)\\&=\min(r_1,\ldots,r_K),\end{aligned}$$

so that the maximum cloud overlap formula (9) applies. We would also like each marginal intra-layer copula C_{T_k,S_k} to be realistic in its representation of the rank dependency of T and S within the layer.

Say our rank generation procedure, to be determined, produces a sample rank vector $\boldsymbol{R}\equiv(U_1,\ldots,U_K,V_1,\ldots,V_K)^T$ and corresponding physical quantities $\boldsymbol{T}\equiv(F_{T_1}^{-1}(U_1),\ldots,F_{T_K}^{-1}(U_K))^T$ and $\boldsymbol{S}\equiv(F_{S_1}^{-1}(V_1),\ldots,F_{S_K}^{-1}(V_K))^T$. One simulation strategy would be to choose a common S rank for each layer, $V_k=V$, with V distributed uniformly on $[0,1]$, but to generate a separate U_k for each layer consistent with specified C_{T_k,S_k}, namely, so that $\text{Fr}(U_k\le u,V\le v)=C_{T_k,S_k}(u,v)$, where the copula on the right hand side has been predetermined from the *observed* rank dependence between T_k and S_k alone.

For example, if C_{T_k,S_k} is a Gaussian copula then, per §11.1 and Appendix B, we may generate ranks from it as $(U_k,V)=(\Phi(\rho_kG_S+\rho'_kG_T),\Phi(G_S))$, where $\rho_k\in(-1,1)$ is the correlation coefficient of Z_{Tk} and Z_{Sk} and $\rho'_k\equiv\sqrt{1-\rho_k^2}\in(0,1]$, and where G_S and G_T are independently distributed random variates $\sim N(0,1)$. Using a common G_S for all layers enforces a maximum rank correlation in S. However, let us also assume that G_T is common to all layers, in order to enforce a measure of rank correlation in T as well, while at the same time maintaining a separate intra-layer Gaussian copula for each layer, characterized by ρ_k. Then

$$\begin{aligned}&C_{\boldsymbol{T},\boldsymbol{S}}(u_1,\ldots,u_K,v_1,\ldots,v_K)\\&\quad=\text{Fr}(U_1\le u_1,\ldots,U_K\le u_K,V\le v_1,\ldots,V\le v_K)\\&\quad=\text{Fr}(G_T\le\min(g_1(V),\ldots,g_K(V)),\\&\qquad\qquad V\le\min(v_1,\ldots,v_K))\\&\quad=\int_0^{\min(v_1,\ldots,v_K)}\Phi(\min(g_1(V),\ldots,g_K(V))\,dV,\end{aligned}$$

DOI: 10.1002/qj

where $g_k(V) \equiv {\rho'_k}^{-1}[\Phi^{-1}(u_k) - \rho_k \Phi^{-1}(V)]$. For $\rho_k = 0$, $\rho'_k = 1$ and $g_k = \Phi^{-1}(u_k)$. If $\rho_k = 0$ for every k, then $\Phi(\min(g_1(V), \ldots, g_K(V)) = \min(u_1, \ldots, u_K)$ and $C_{\boldsymbol{T},\boldsymbol{S}}(\boldsymbol{u}, \boldsymbol{v}) = \min(u_1, \ldots, u_K) \min(v_1, \ldots, v_K)$, i.e., each of T and S is independently maximally rank-correlated. For general ρ_k, note that $\lim_{u_k \to 1} g_k(V) = \infty$ and so $C_{\boldsymbol{S}}(\boldsymbol{v}) = C_{\boldsymbol{T},\boldsymbol{S}}(1, \ldots, 1, \boldsymbol{v}) = \min(v_1, \ldots, v_K)$, as required.

References

Chakak A, Koehler KJ. 1995. A strategy for constructing multivariate distributions. *Commun. Statist. — Simula.* **24**: 537–550.

Cherubini U, Luciano E, Vecchiato W. 2004. *Copula methods in finance*. John Wiley & Sons, Ltd.

Chou MD, Suarez MJ. 1999. A shortwave radiation parameterization for atmospheric studies. Technical Report 15(104606), National Aeronautics and Space Administration.

Chou MD, Suarez MJ, Ho CH, Yan MMH, Lee KT. 1998. Parameterizations for cloud overlapping and shortwave single-scattering properties for use in general circulation and cloud ensemble models. *J. Clim.* **11**: 202–214.

Chou MD, Suarez MJ, Liang XZ, Yan MMH. 2001. A thermal infrared radiation parameterization for atmospheric studies. Technical Report 19(104606), National Aeronautics and Space Administration.

Dee DP, da Silva AM. 1999. Maximum-likelihood estimation of forecast and observation error covariance parameters. Part I: Methodology. *Mon. Wea. Rev.* **127**: 1822–1834.

Dee DP, da Silva AM. 2003. The choice of variable for atmospheric moisture analysis. *Mon. Wea. Rev.* **131**: 155–171.

Dee DP, Gaspari G, Redder C, Rukhovets L, da Silva AM. 1999. Maximum-likelihood estimation of forecast and observation error covariance parameters. Part II: Applications. *Mon. Wea. Rev.* **127**: 1835–1849.

Gaspari G, Cohn SE. 1999. Construction of correlation functions in two and three dimensions. *Q. J. R. Meteor. Soc.* **125**: 723–757.

Gaspari G, Cohn SE, Guo J, Pawson S. 2006. Construction and application of covariance functions with variable length-fields. *Q. J. R. Meteor. Soc.* **132**: 1815–1838.

Geleyn JF, Hollingsworth A. 1979. An economical analytic method for the computation of the interaction between scattering and line absorption of radiation. *Beitr. Phys. Atmos.* **52**: 1–16.

Genz A. 1992. Numerical computation of multivariate normal probabilities. *J. Comp. Graph. Stat.* **1**: 141–149.

Hogan RJ, Illingworth AJ. 2000. Deriving cloud overlap statistics from radar. *Q. J. R. Meteorol. Soc.* **126**: 2903–2909.

Jakob C, Klein SA. 1999. The role of vertically varying cloud fraction in the parameterization of microphysical processes in the ECMWF model. *Q. J. R. Meteorol. Soc.* **125**: 941–965.

Larson VE, Wood R, Field PR, Golaz JC, Vonder Haar TH, Cotton WR. 2001. Small-scale and mesoscale variability of scalars in cloudy boundary layers: One-dimensional probability density functions. *J. Atmos. Sci.* **58**: 1978–1994.

Li J, Barker HW. 2002. Accounting for unresolved clouds in a 1D infrared radiative transfer model. part II: Horizontal variability of cloud water path. *J. Atmos. Sci.* **59**: 3321–3339.

Mace GG, Benson-Troth S. 2002. Cloud-layer overlap characteristics derived from long-term cloud radar. *J. Climate* **15**: 2505–2515.

Nelson RB. 2006. *An Introduction to Copulas*. Springer.

Norris PM, da Silva AM. 2007. Assimilation of satellite cloud data into the GMAO Finite Volume Data Assimilation System using a parameter estimation method. *J. Atmos. Sci.* Accepted for publication.

Oreopoulos L, Khairoutdinov M. 2003. Overlap properties of clouds generated by a cloud resolving model. *J. Geophys. Res.* **108**: 4479. Doi:10.1029/2002JD003329.

Pincus R, Hannay C, Klein SA, Xu KM, Hemler R. 2005. Overlap assumptions for assumed-PDF cloud schemes in large scale models. *J. Geophys. Res.* **110**. Art. No. D15S09.

Räisänen P, Barker HW. 2004. Evaluation and optimization of sampling errors for the Monte Carlo Independent Column Approximation. *Q. J. R. Meteor. Soc.* **130**: 2069–2085.

Räisänen P, Barker HW, Cole JNS. 2005. The Monte Carlo independent column approximation's conditional random noise: Impact on simulated climate. *J. Climate* **18**: 4715–4730.

Räisänen P, Barker HW, Khairoutdinov MF, Li J, Randall DA. 2004. Stochastic generation of subgrid-scale cloudy columns for large-scale models. *Q. J. R. Meteor. Soc.* **130**: 2047–2068.

Sancetta A. 2005. Copula based monte carlo integration in financial problems. Cambridge Working Papers in Economics 0506, Faculty of Economics (formerly DAE), University of Cambridge. Available at http://ideas.repec.org/p/cam/camdae/0506.html.

Smith RNB. 1990. A scheme for predicting layer clouds and their water content in a general circulation model. *J. Q. R. Meteorol. Soc.* **116**: 435–460.

Tian L, Curry JA. 1989. Cloud overlap statistics. *J. Geophys. Res.* **94**: 9925–9935.

Tompkins AM. 2002. A prognostic parameterization for the subgrid-scale variability of water vapor and clouds in large-scale models and its use to diagnose cloud cover. *J. Atmos. Sci.* **59**: 1917–1942.

Tompkins AM. 2003. Impact of temperature and humidity variability on cloud cover assessed using aircraft data. *Q. J. R. Meteorol. Soc.* **129**: 2151–2170.

Xu KM, Randall DA. 1996. Evaluation of statistically based cloudiness parameterizations used in climate models. *J. Atmos. Sci.* **53**: 3103–3119.

Zeng X, Tao WK, Zhang M, Peters-Lidard C, Lang S, Simpson J, Kumar S, Xie S, Eastman JL, Shie CL, Geiger JV. 2007. Evaluating clouds in long-term cloud-resolving model simulations with observations. *J. Atmos. Sci.* In Press.

DOI: 10.1002/qj